地震研究所彙報
Bull. Earthq. Res. Inst.
Univ. Tokyo
Vol. 74 (1999) pp. 267-285

ASOBOI 97: Aso Seismic Observation with Broadband Instruments in 1997

Mare YAMAMOTO[1], Hitoshi KAWAKATSU[1], Satoshi KANESHIMA[2], Takashi IIDAKA[1], Jun OIKAWA[1], Shingo WATADA[1], Yuichi MORITA[1], Takehiko MORI[3], Tomoki TSUTSUI[3], Yasuaki SUDO[3], Makoto YOSHIKAWA[3], Takeshi HASHIMOTO[3] and Makoto NAKABO[3]

[1] Earthquake Research Institute, University of Tokyo
[2] Faculty of Sciences, Tokyo Institute of Technology
[3] Aso Volcanological Laboratory, Faculty of Science, Kyoto University

Abstract

In August 1997, we deployed a total of 24 broadband three-component velocity seismometers temporarily around Aso volcano in Kyushu, Japan. Most of these stations were located within 1 km of the first crater of Naka-dake and provided good azimuthal coverage to constrain the geometry of the source region of long-period (15 s) tremors (LPTs). The spatial pattern of the observed LPTs amplitude reveals that the source of LPTs consists of an isotropic expansion (contraction) and an inflation (deflation) of an inclined tensile crack almost parallel to the chain of craters of Naka-dake (Yamamoto *et al.*, 1999). This report summarizes details of the observations, as well as some of the characteristics of the observed data from the ASOBOI 97 expedition.

Key words: broadband seismometer, volcanic tremor, crack, Aso

1. Introduction

Seismic signals observed in and around volcanoes contain many complicated wave phenomena. A volcanic tremor is a type of seismic event that occurs only near volcanoes. Since its first observation by Omori (1911, 1912), there have been many speculations about the source mechanism of volcanic tremors and numerous reports of observations at various volcanoes (e.g. Chouet, 1996).

At Aso Volcano in Kyushu, Japan, volcanic signals with unusually long period (about 7 sec) have been observed since its discovery by Sassa (1935), and recent advances in broadband seismometry revealed the existence of signals with an even longer period (i.e.~15 sec) (Kaneshima *et al.*, 1996; Kawakatsu *et al.*, 1999). They are called "long period tremors (LPTs)" by Kaneshima *et al.* (1996) (signals with a period of 7 sec are named "the volcanic micro-tremors of the second kind" by Sassa (1935)). A typical LPT has a short duration of several tens of seconds, and its spectrum shows peaks at about 15 sec, 7.5 sec, 5 sec, and 3 sec (Fig. 1). LPTs are observed even when there is no surface activity, and they have been emitted from the volcano continually at least over the last several years.

Previously we attempted to locate the source of LPTs and to understand their

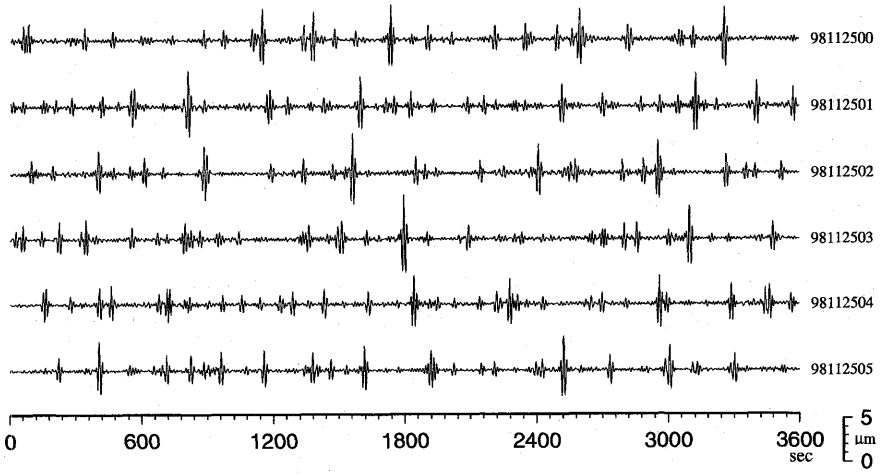

(a)

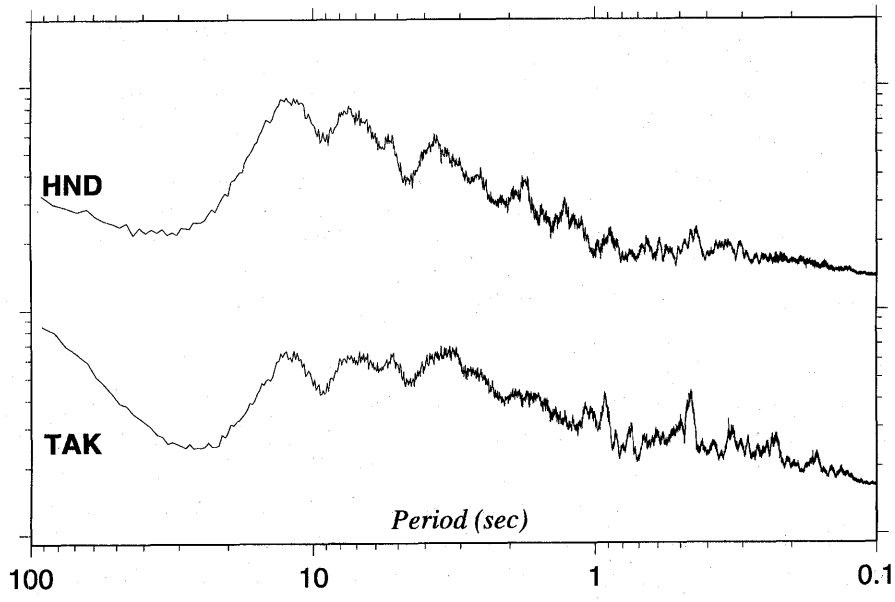

(b)

Fig. 1. (a) Typical long-period seismograms observed at Aso. Vertical component band-pass filtered (10–30 sec) displacement seismograms at HND for six hours starting at 00: 00 on Nov. 25, 1998 (JST) are shown. LPTs are seen as isolated wave packets. Note that these records are not observed during ASOBOI97. (b) Amplitude spectrum of LPTs. Spectra of LPTs for stations HND and TAK are shown. These spectra are obtained by stacking 176 FFT spectra for 15-minute long raw velocity seismograms of March 22–23, 1998. Each spectrum shows several peaks at about 15 sec, 7.5 sec, 5 sec, and 3 sec.

mechanism using methods such as 'waveform semblance' (Kawakatsu *et al.*, 1999) and point source moment tensor waveform inversion (Legrand *et al.*, 1999). We have shown that the source of LPTs (centroid location of moment release) is at a few hundred meters southwest of the first crater at a depth of 1-1.5 km; The resolved seismic moment tensor corresponds to a combination of isotropic expansion (contraction) and inflation (deflation) of a vertical crack, but the significance of the crack component was questionable because of the limited station coverage.

The purpose of our deployment of a dense broadband seismic network in 1997 was to constrain the geometry of this postulated crack component using the spatial pattern of LPT amplitudes.

2. ASOBOI 97

From August 24 to 30, 1997, we deployed a broadband seismic network named ASOBOI 97[1] (Aso Seismic Observation with BrOadband Instruments 97) around Naka-dake of Aso volcano. The network included ten Guralp CMG-3T (represnted by

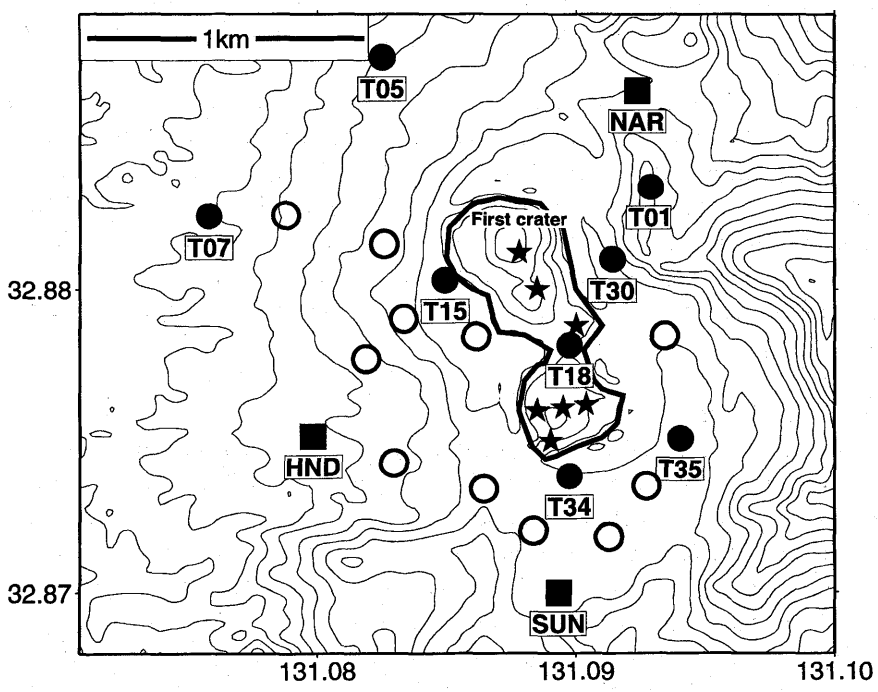

Fig. 2. ASOBOI 97. Aso volcano is located in central Kyushu, Japan. Filled circles and open circles represent stations with CMG-3T and CMG-40T, respectively. Three permanent stations are represented by squares. Star indicates the location of the active fumarole of the first crater of Naka-dake. Most of the stations are located within 1 km from the first crater. Two stations (KSR and T00 in Table 1) are located outside this figure.

[1] In the local dialect, "aso-boi" means 'let's play together'

filled-circles in Fig. 2) and three Guralp CMG-40T (open-circles in Fig. 2) seismometers with natural periods of 100 sec and 30 sec, respectively. Each CMG-3T sensor was placed in a 0.5 m-deep hole and entirely buried after installation (Photo. 1). Some of CMG-40T sensors were buried and the others were placed on the ground surface directly. Their velocity outputs were recorded continuously using portable recorders (Data Mark LS 8000 WD for CMG-3T, Data Mark LS 8000 SH for CMG-40T) whose clocks were locked with GPS. Due to the limited storage of LS 8000 SH, and in order to avoid artificial noise, recording for CMG-40T was restricted to overnight from 22: 00 to 07: 00 (JST); After each one-night session, three stations with CMG-40T changed their locations, and a total of eleven stations were set up during August 26–29. Besides this temporary seismic-network, our analysis also includes data recorded at permanemt stations HND (with CMG-3T), SUN (with Streckkeisen STS-2), and NAR (STS-2). Sensor orientations of the stations of the network were obtained by field measurements with compasses first, and later measured using a gyroscope. Station calibration (in terms of amplitude) and sensor orientations were also checked by comparing three-component waveforms and amplitudes of a filtered (10–30 sec) teleseismic surface wave from a Mw 5.9 earthquake occurred in Vanuatu region on August 27.

Twenty-two of these 24 stations (including three permanent stations) are located within 1.5 km from the first crater of Naka-dake (for example, T 18 station was set at the bottom of the second crater which is only 250 m from the active fumarole of first crater), and provided good azimuthal coverage (Fig. 2). Further details of the network are given in Table 1. Although a similar broadband seismic network around Aso volcano was operated in 1994 (Kaneshima *et al.*, 1996; Kawakatsu *et al.*, 1999), their stations were more sparse and more distant from the crater than this network.

3. Data

3.1 Observed data

Fig. 3 shows examples of the ground displacement signals after integrating and applying a 10–30 sec band-pass filter to the observed raw velocity data to eliminate microseismic noise in which the long period signals are covered. On filtered records, LPTs are seen as isolated wave packets of only a few cycles. Note that during the observation we recorded these LPT signals continually, although Aso volcano was not so active and there was no major surface activity around the crater. Visual comparison of these filtered signals shows strong similarity of LPTs at all stations and at all events, although the signal amplitudes vary from event to event. The fact that the waveforms of all events are almost identical suggests the source process of LPTs is repetitive and not so destructive. On the other hand, the similarity in shape from station to station is attributed to the fact that static displacement dominates in such a near-field (Legrand *et al.*, 1999). All these observations are consistent with our earlier observation (Kaneshima *et al.*, 1996; Kawakatsu *et al.*, 1999).

3.2 Stacking of LPTs

The most remarkable observation is the spatial variation of LPT amplitudes (Fig. 3).

(a)

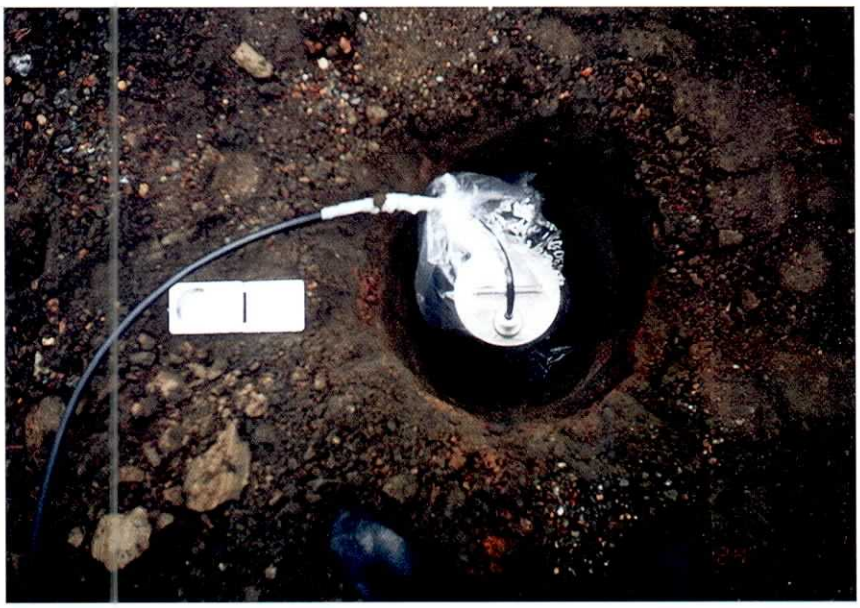

(b)

Photo. 1. Observation scenery. (a) : Station T18. The depression seen above is the first crater. (b) : Installation of a CMG-3T seismometer in a hole.

Table 1. Network information.

Station	Operation	Sensor	Recorder	Sampling frequency	Longitude (deg)	Latitude (deg)	Elevation (km)
T00	8/25-30	CMG-3T	LS8000WD	100 → 20Hz	131.1033	32.8933	0.98
T01	8/25-30	CMG-3T	LS8000WD	100 → 20Hz	131.0929	32.8834	1.37
T05	8/24-30	CMG-3T	LS8000WD	100 → 20Hz	131.0825	32.8876	1.17
T07	8/24-30	CMG-3T	LS8000WD	100 → 20Hz	131.0758	32.8824	1.12
T15	8/24-30	CMG-3T	LS8000WD	100 → 20Hz	131.0849	32.8803	1.26
T18	8/24-30	CMG-3T	LS8000WD	100 → 20Hz	131.0898	32.8782	1.24
T30	8/24-30	CMG-3T	LS8000WD	100 → 20Hz	131.0914	32.8810	1.28
T34	8/25-30	CMG-3T	LS8000WD	100 → 20Hz	131.0898	32.8738	1.25
T35	8/24-30	CMG-3T	LS8000WD	100 → 20Hz	131.0940	32.8751	1.25
KSR	8/24-30	CMG-3T	LS8000WD	100 → 20Hz	131.0558	32.8825	1.24
I12	8/28-29	CMG-40	LS8000SH	100 → 20Hz	131.0819	32.8777	1.10
I13	8/28-29	CMG-40	LS8000SH	100 → 20Hz	131.0833	32.8790	1.24
I17	8/28-30	CMG-40	LS8000SH	100 → 20Hz	131.0861	32.8784	1.27
I21	8/25-27	CMG-40	LS8000SH	100 → 20Hz	131.0884	32.8720	1.24
I22	8/25-27	CMG-40	LS8000SH	100 → 20Hz	131.0864	32.8734	1.24
I23	8/25-27	CMG-40	LS8000SH	100 → 20Hz	131.0829	32.8743	1.19
I31	8/27-28	CMG-40	LS8000SH	100 → 20Hz	131.0934	32.8785	1.25
I32	8/27-28	CMG-40	LS8000SH	100 → 20Hz	131.0927	32.8735	1.24
I33	8/27-28	CMG-40	LS8000SH	100 → 20Hz	131.0913	32.8718	1.24
I41	8/29-30	CMG-40	LS8000SH	100 → 20Hz	131.0826	32.8815	1.22
I42	8/29-30	CMG-40	LS8000SH	100 → 20Hz	131.0788	32.8824	1.16
HND	continuous	CMG-3T	REFTEK	20Hz	131.0798	32.8752	1.14
SUN	continuous	STS-2	REFTEK	20Hz	131.0893	32.8700	1.24
NAR	continuous	STS-2	REFTEK	20Hz	131.0924	32.8865	1.27
1st crater	——	——	——	——	131.0879	32.8819	1.15

Because of the slow fall-off of the anti-alias filter used in LS8000WD and LS8000SH, data streams from CMG-3T were recorded at a sampling rate of 100 Hz, and, after their collection, resampled at 20 samples/sec after applying the FIR filter whose coefficients are same as those used in PASSCAL instruments installed at HND and SUN. "first crater" in this table points at the location represented as "11547" on the volcanic base map by Geographical Survey Institute, Japan (1982).

However, signal amplitude of each LPT measured directly from records may be polluted by random noise. Indeed, the quality of the observed raw data is variable, and the relatively small amplitude of LPTs during our observation makes the signal-to-noise ratio low. To avoid the effects of noise, rather than using observed raw signals, we use stacked signals with an improved signal-to-noise ratio to see this pattern of amplitudes in more detail. We determine the reference times for stacking as follows (Fig. 4);

1. first prepare a "reference LPT" waveform by stacking 10 filtered (10-30 sec) LPTs observed at HND (our reference station).

2. then cross-correlate the filtered seismograms observed at HND with these reference LPTs and determine the maximum cross-correlation coefficients and the

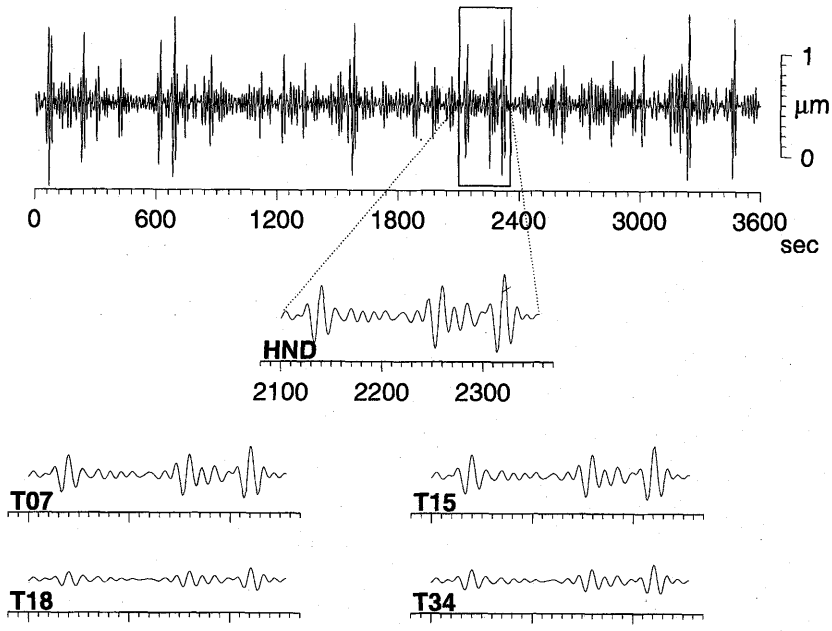

Fig. 3. Observed LPTs. Top: Vertical component band-pass filtered (10–30 sec) displacement seismogram for one hour starting at 01: 00 on Aug. 26, 1997 (JST). Bottom: Examples of seismograms observed at different stations. All traces are drawn in the same scale and for same time window. These seismograms are obtained by integrating the observed velocity records.

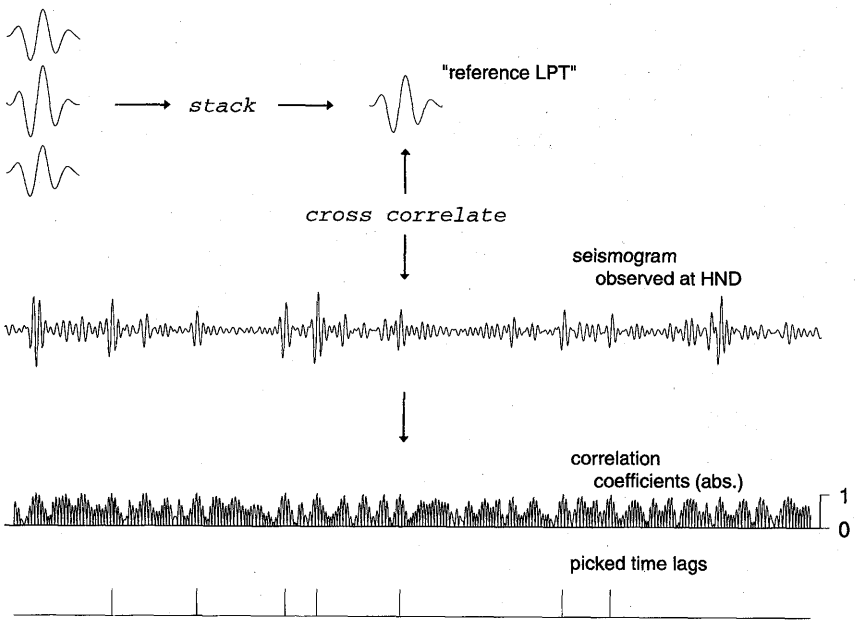

Fig. 4. Schematic illustration of the picking procedure (see text for details).

corresponding time lags.

3. when the correlation coefficient exceeds 0.98, the corresponding time lag is assigned to the reference time for stacking

This picking calculation is done against data obtained during the period when stations with CMG-40T (hereafter noted as mobile array) were in operation (i.e. from 22: 00 to 07: 00 of August 26–29). After this procedure, we visually check the waveforms around these time marks and finally select 340 reference times. Once the reference times are determined, signals at each station are stacked using this time lag

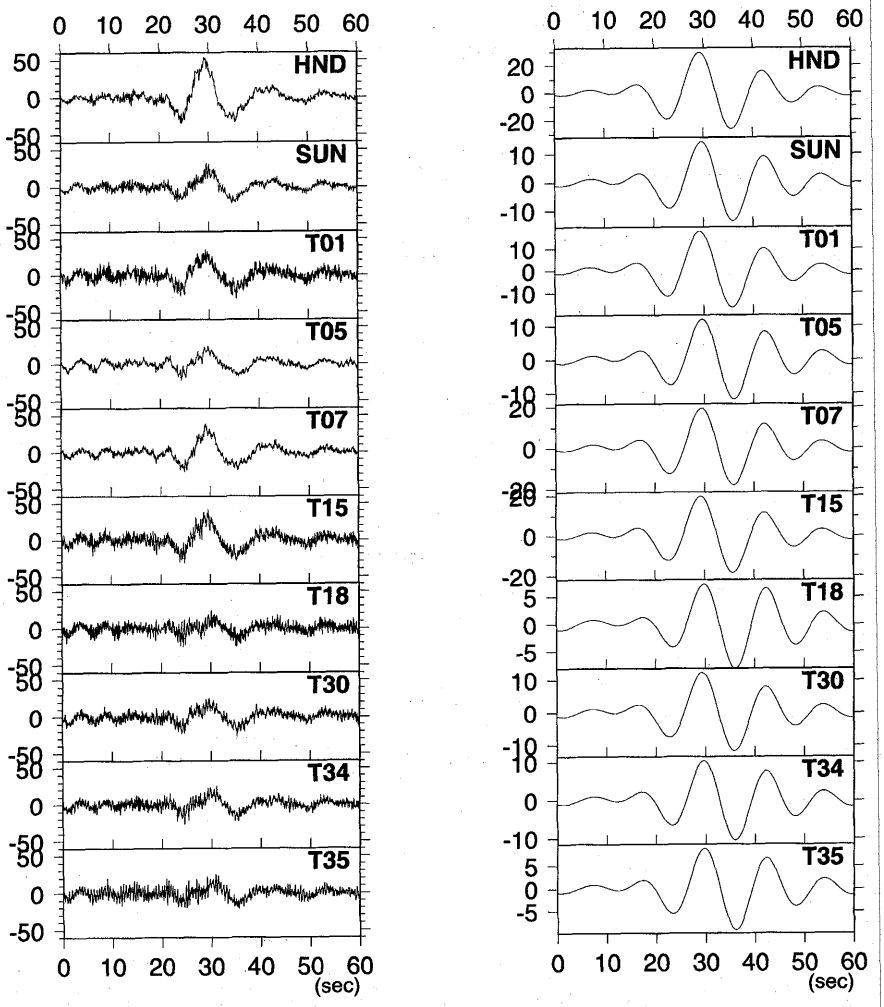

Fig. 5. Results of stacking. (a) Samples of stacked LPTs obtained by stacking 100 records. Left: Raw stacked data (all traces are drawn to the same scale). Right: Bandpass filtered (10–30 sec) stacked data (each trace is scaled by its maximum to show the similarity of the waveforms).

information. Note that stacking for each station is performed using the same time marks, and signals are neither normalized nor filtered prior to stacking. For each stacked trace, peak-to-peak amplitudes are measured after applying a 10–30 sec band-pass filter, and then relative amplitudes to that of HND are estimated. Examples of the results of stacking are shown in Fig. 5. To estimate the standard errors of obtained relative amplitudes, we use the bootstrap method (Efron and Tibshirani, *1993*); The stacking described above in which we randomly selected events is repeated 100 times. Resultant values of the standard errors are listed in Table 2. Due to

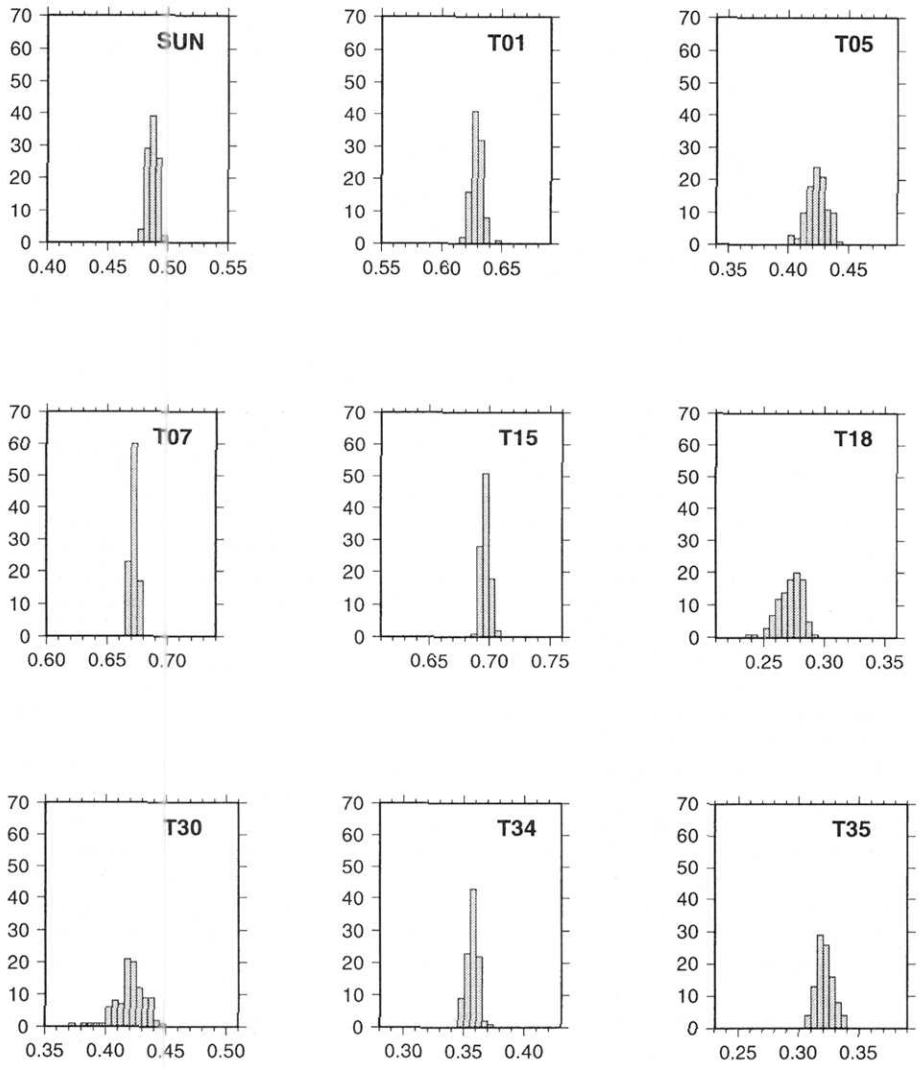

Fig. 5. Results of stacking. (b) Histogram of the obtained relative amplitudes of 100 stacked LPTs (vertical component).

the low signal-to-noise ratio, we could not obtain reliable relative amplitudes of horizontal components for stations with CMG-40T (i.e., stations of the mobile array).

3.3 Amplitude variation

Obtained relative amplitudes of the vertical component are listed in Table 2, and their spatial pattern is illustrated in Fig. 6 (a). The pattern shows the characteristic where by amplitudes are small along the chain of craters of Naka-dake, and are large around the southwest of the edifice. The smaller amplitude observed at the bottom of the second crater, which is only a few hundred meters away from the first crater, was rather unexpected (see the signal at T 18 in Fig. 3). Fig. 6 (b) also shows a two-dimensional projection of this spatial pattern of amplitude onto a vertical plane perpendicular to the chain of craters. On this projection, the amplitudes at stations within 0.35 km from the line **A-A'** (between two broken lines) show a simple pattern. This pattern invokes the idea of a crack-like source of LPTs with a node along the chain of craters. In addition, from the fact that amplitudes at all stations have the same sign, we expect that the source of LPTs consists of not only an inflation (deflation) of a crack but also an isotropic expansion (contraction).

4. Detection of a crack-like conduit

We try to explain the obtained spatial pattern of the amplitude of LPT using a

Table 2. Relative amplitudes.

Station	Longitude (deg)	Latitude (deg)	Elevation (km)	Relative amplitude (HND = 1)		
				vertical (UD)	horizontal (NS)	horizontal (EW)
T01	131.0929	32.8837	1.37	0.62 ± 0.01	-0.45 ± 0.16	-0.41 ± 0.06
T05	131.0825	32.8876	1.17	0.42 ± 0.01	-0.38 ± 0.12	-0.11 ± 0.07
T07	131.0758	32.8824	1.12	0.67 ± 0.01	-0.56 ± 0.07	0.66 ± 0.02
T15	131.0849	32.8803	1.26	0.69 ± 0.01	-0.28 ± 0.06	-0.23 ± 0.03
T18	131.0898	32.8782	1.24	0.28 ± 0.01	-0.30 ± 0.07	-0.26 ± 0.03
T30	131.0914	32.8810	1.28	0.43 ± 0.01	-0.17 ± 0.09	-0.16 ± 0.03
T34	131.0898	32.8738	1.25	0.36 ± 0.01	-0.21 ± 0.09	-0.35 ± 0.08
T35	131.0940	32.8751	1.25	0.31 ± 0.01	-0.25 ± 0.11	-0.26 ± 0.07
I12	131.0819	32.8777	1.10	1.10 ± 0.02	—	—
I13	131.0833	32.8790	1.24	1.04 ± 0.09	—	—
I17	131.0861	32.8784	1.27	0.74 ± 0.06	—	—
I22	131.0864	32.8734	1.24	0.75 ± 0.02	—	—
I23	131.0829	32.8743	1.19	0.88 ± 0.07	—	—
I41	131.0829	32.8815	1.22	1.00 ± 0.05	—	—
I42	131.0788	32.8824	1.16	0.79 ± 0.02	—	—
HND	131.0798	32.8752	1.14	1.00	1.00	1.00
SUN	131.0893	32.8700	1.15	0.48 ± 0.01	0.63 ± 0.04	-0.23 ± 0.03
NAR	131.0924	32.8865	1.27	0.60 ± 0.01	—	—
1st crater	131.0879444	32.88194444	1.15	—	—	—

As the error, the standard errors of 100 stacked LPTs estimated by Bootstrap method are listed in this table. The standard errors are calculated by $\sqrt{\frac{1}{n-1}\sum(x-\frac{1}{n}\sum x)^2}$.

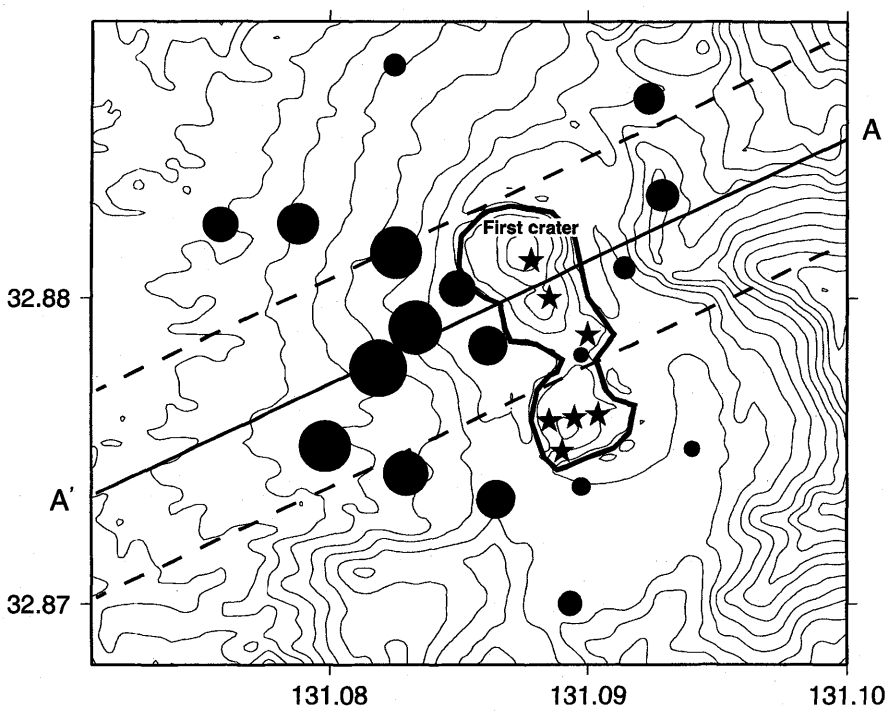

(a)

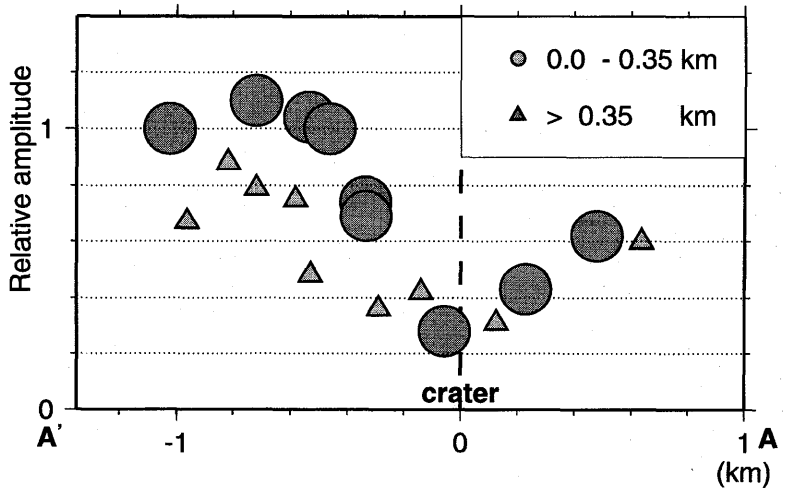

(b)

Fig. 6. Spatial pattern of the relative amplitudes of vertical components and their two-dimensional projection. (a) radius of each circle represents the relative signal amplitude at each station.

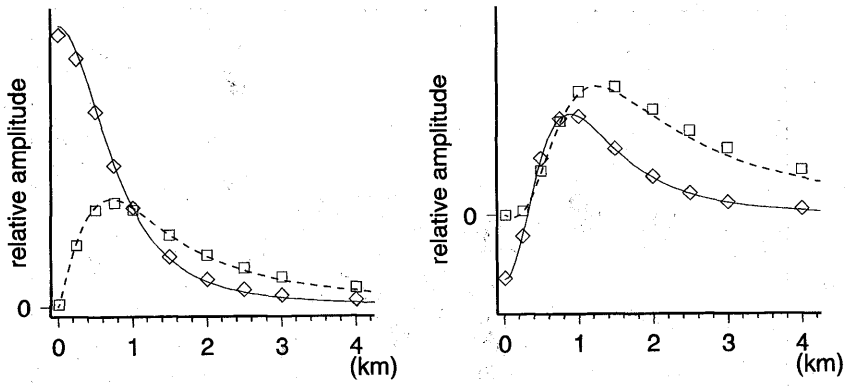

Fig. 7. Comparison of static displacement and bandpass filtered signal in the near-field. Left: Isotropic point source at a depth of 1 km. Right: Vertical tensile point source at a depth of 1 km. Solid line, dashed-line, diamond, and square represent the vertical and radial components of the static displacement and bandpass filtered signal, respectively. Amplitudes are normalized by the amplitude of the vertical component at a distance of 1 km.

simple model, which consists of an isotropic point source and an inclined tensile crack by a grid-search calculation. In our model search, we assume that the amplitude of the long period signal observed in the near-field is proportional to that of static displacement (Legrand *et al.*, 1999), and use a code of Okada (1992) to calculate the static displacement due to a source in a half space. In Fig. 7, the amplitude variation of the static displacement and its band-pass (10–30 sec) filtered version due to point sources is shown as a function of the epicentral distance in the near-field. The synthetic signals used for the band-pass filtered signals are obtained by convolving a step function with a Green's function for a homogeneous half space (Johnson, 1974).

Analyses of these data are given in Yamamoto *et al.* (1999) where the presence of a crack-like conduit beneath the active crater is clearly demonstrated. Table 3 and Figs. 8 and 9 summarize the results of Yamamoto *et al.* (1999).

5. Summary

From a dense broadband seismic observation named ASOBOI 97, the presence of a crack-like conduit beneath the active crater at Aso volcano was revealed by Yamamoto *et al.* (1999). The spatial variation of LPT amplitude was used to constrain the geometrical parameters of the LPT source. Similar observations at other volcanoes may reveal unraveled sub-surface structures under active volcanoes.

Acknowledgments

We thank Yuji Nishi and Toshiyuki Tosha of Geological Survey of Japan for allowing us to use their broadband observation system. Comments by two anony-

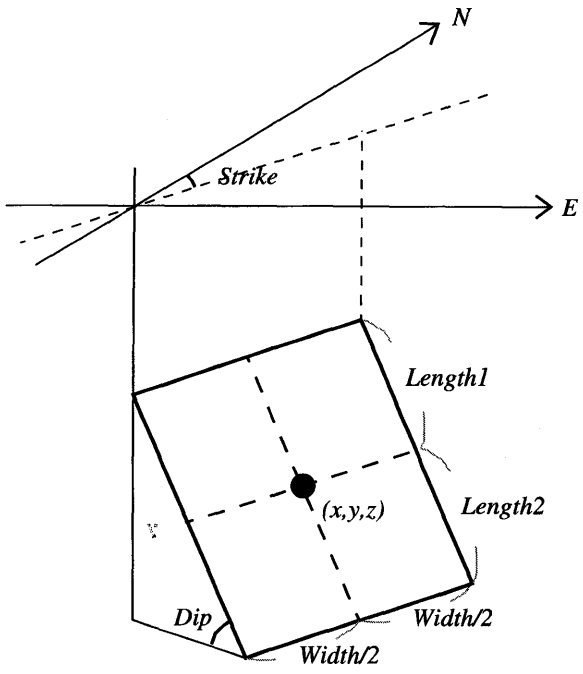

Fig. 8. Definition of the parameters for the model grid-search.

mous reviewers improved the manuscript. This research was supported by Japanese Monbusho under the grant No. 09304043.

Appendix

To represent the LPT activity of Aso volcano during ASOBOI97, band-pass filtered records at HND station are shown.

References

CHOUET, B., 1984, Long-period volcano seismicity: its source and use in eruption forecasting, *Nature*, **380**, 309-316.

EFRON, B., R.J. TIBSHIRANI, 1993, An Introduction to the Bootstrap, *Chapman & Hall/CRC*.

JOHNSON, L.R., 1974, Green's function for Lamb's problem, *Geophys. J. Roy. Astr. Soc.*, **37**, 99-131.

KANESHIMA, S., KAWAKATSU, H., MATSUBAYASHI, H., SUDO, Y., TSUTSUI, T., OHMINATO, T., ITO, H., UHIRA, K., YAMASATO, H., OIKAWA, J., TAKEO, M. and IIDAKA, T., 1996, Mechanism of phreatic eruptions at Aso volcano inferred from near-field broadband seismic observations, *Science*, **273**, 642-645.

KAWAKATSU, H., KANESHIMA, S., MATSUBAYASHI, H., OHMINATO, T., SUDO, Y., TSUTSUI, T. UHIRA, K., YAMASATO, H., ITO, H., LEGRAND, D., 1999, Aso94: Aso seismic observation with broadband instruments, *J. Volcanol. Geotherm. Res.*, in press.

LEGRAND, D., KANESHIMA, S. and KAWAKATSU, H., 1999, Moment tensor analysis of near field

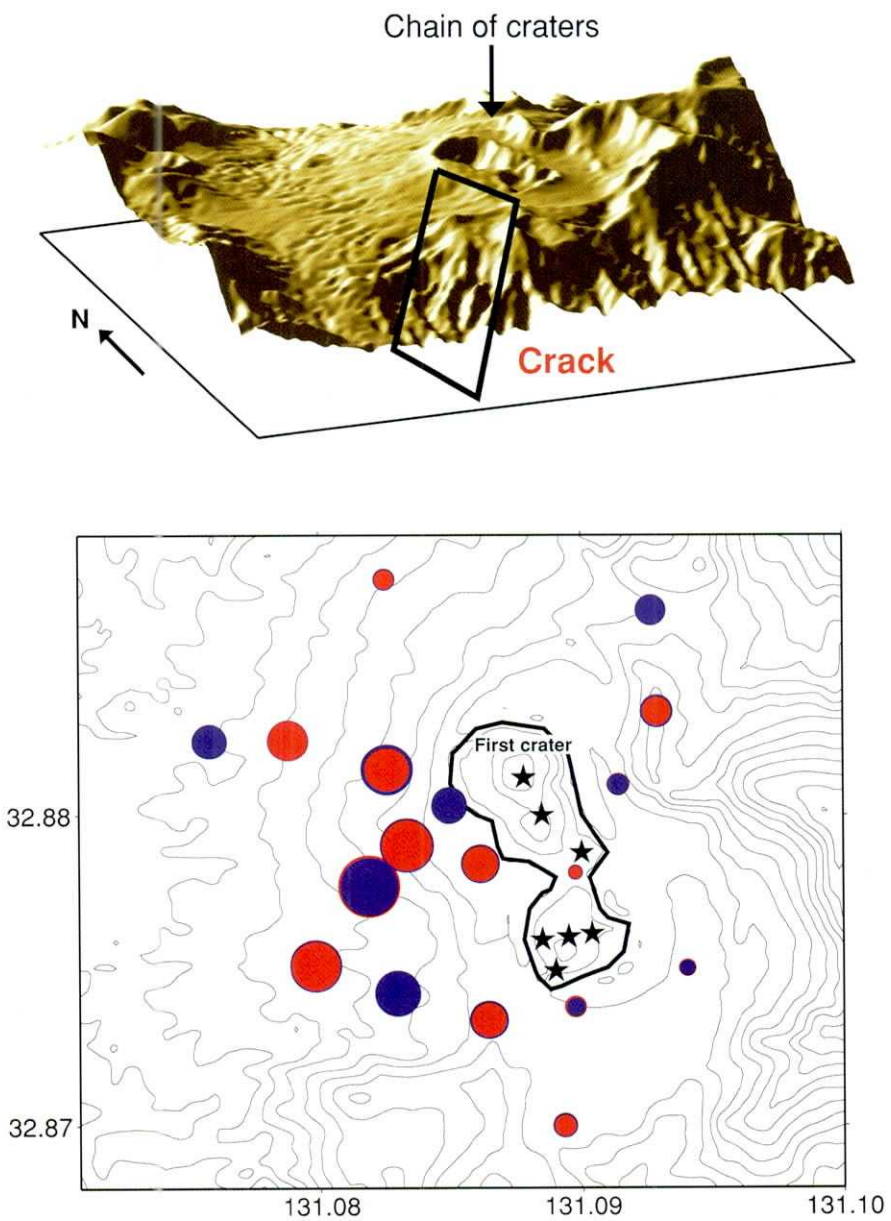

Fig. 9. Image of obtained model and expected signal amplitude. Top: Image of our isotropic point source plus tensile crack. The crack is almost parallel to the chain of craters. Bottom: The observed and the model-predicted amplitudes are respectively represented as red and blue circles whose radii are proportional to the values of the amplitudes. In this figure, a smaller circle is put onto a larger one, thus the width of the ring represents the misfit, which is very small.

Table 3. Model (Yamamoto et al. (1999)).

	best fit model parameter		reasonable parameter range
isotropic point source	north	: -0.2 km	-0.3 ~ -0.1 km
	east	: -0.1 km	-0.2 ~ -0.1 km
	depth	: 1.8 km	1.6 ~ 1.8 km
tensile crack	dip	: 85°	83 ~ 86°
	strike	: -28°	-31 ~ -26°
	width	: 1.0 km	0.8 ~ 1.2 km
	length	: 1.5 km (upper part)	> 1.4 km (upper part)
		: 1.0 km (lower part)	0.4 ~ 1.4 km (lower part)

broadband waveforms observed at Aso volcano, Japan, *J. Volcanol. Geotherm. Res.*, in press.

MOGI, K., 1958, Relations between the eruptions of various volcanoes and the deformation of the ground surface around them, *Bull. Earthquake Res. Inst., Univ. Tokyo*, **36**, 99–134.

OKADA, Y., 1992, Internal deformation due to shear and tensile faults in a half-space, *Bull. Seism. Soc. Am.*, **82**, 1018–1040.

OMORI, F., 1911, The Usu-san eruption and earthquake and elevation phenomena, *Imp. Earthquake Invest. Comm.*, **5**, 1–38.

OMORI, F., 1912, The eruptions and earthquakes of the Asama-Yama, Part I-V, *Imp. Earthquake Invest. Comm.*, **6**, 1–456.

SASSA, K., 1935, Volcanic micro-tremors and eruption-earthquakes (Part 1 of the geophysical studies on the volcano Aso), *Mem. Coll. Sci. Kyoto Univ. Series A*, **18**, 255–293.

YAMAMOTO, M., H. KAWAKATSU, S. KANESHIMA, T. MORI, T. TSUTSUI, Y. SUDO, Y. MORITA, 1999, Detection of a crack-like conduit beneath the active crater at Aso volcano, Japan, *Geophys. Res. Lett.*, **26**, 3677–3680.

(Received November 11, 1999)
(Accepted February 16, 2000)

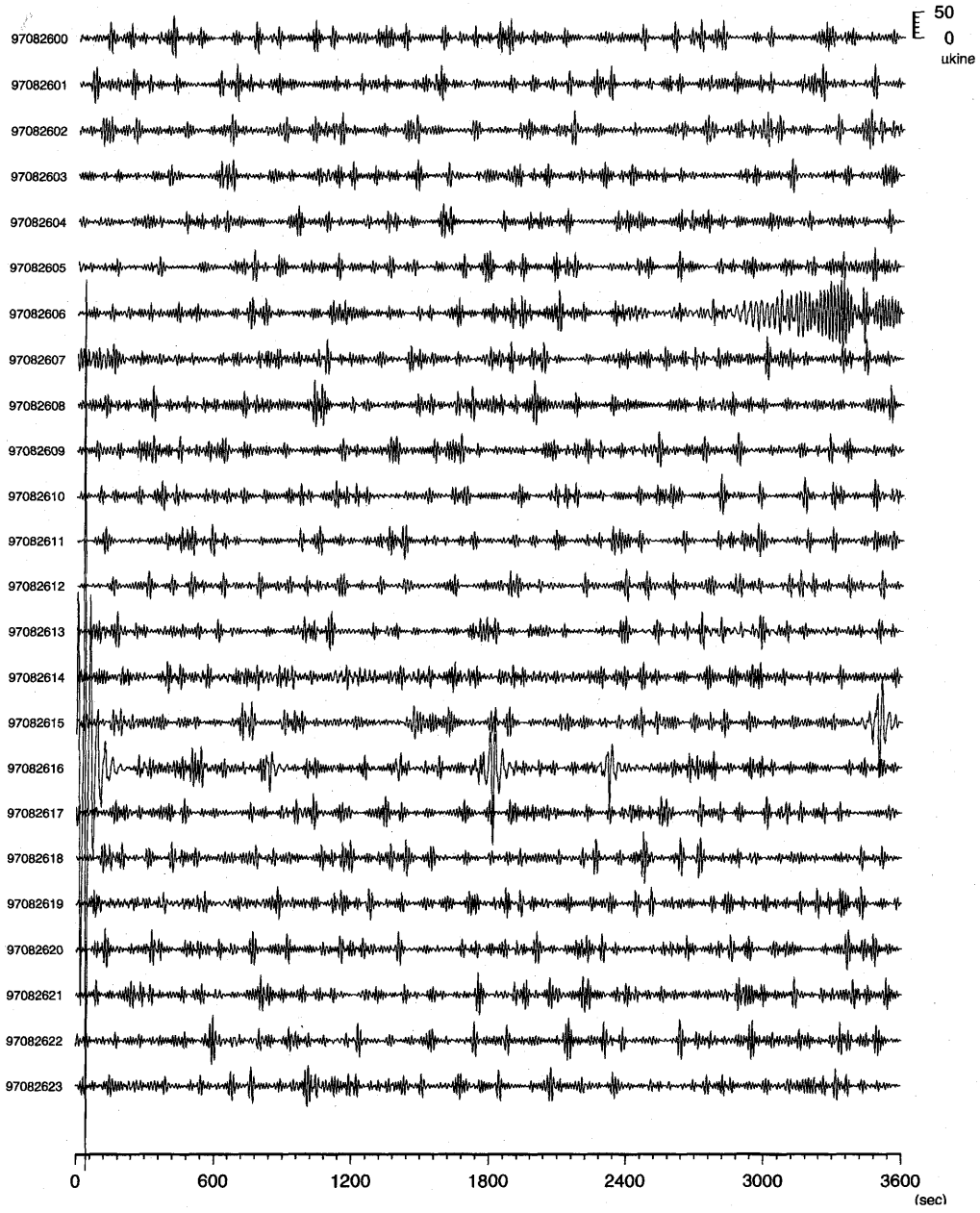

Fig. A. Representative LPT seismograms of ASOBOI97. Vertical component band-pass filtered (10–30 sec) velocity seismograms at HND on (1) Aug. 26, 1997 (JST), (2) Aug. 27, 1997 (JST), (3) Aug. 28, 1997 (JST), and (4) Aug. 29, 1997 (JST). Horizontal scale is one hour and the beginning time of each trace is indicated at the left of the plot.

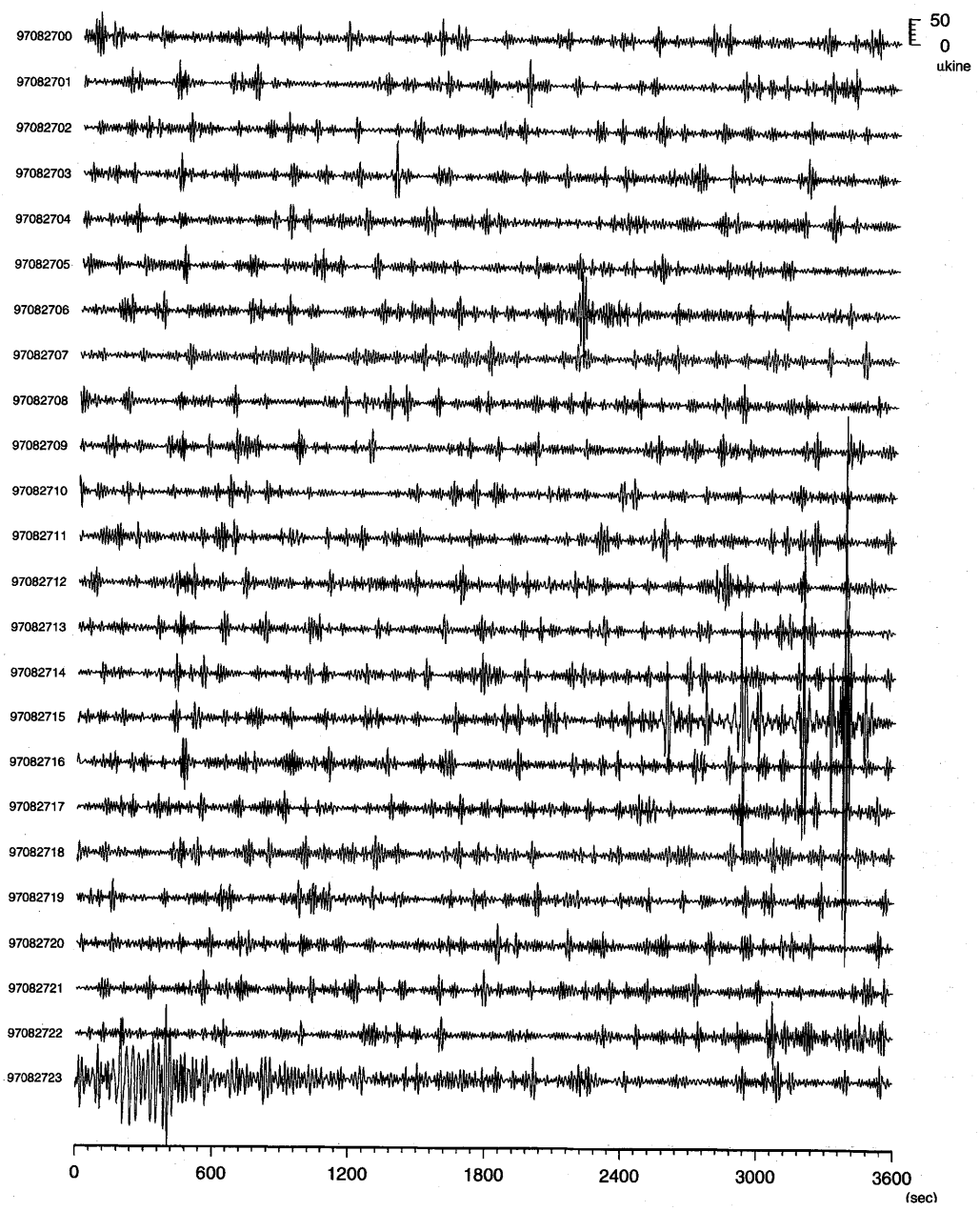
97082700
97082701
97082702
97082703
97082704
97082705
97082706
97082707
97082708
97082709
97082710
97082711
97082712
97082713
97082714
97082715
97082716
97082717
97082718
97082719
97082720
97082721
97082722
97082723
50
0
ukine
0
600
1200
1800
2400
3000
3600
(sec)

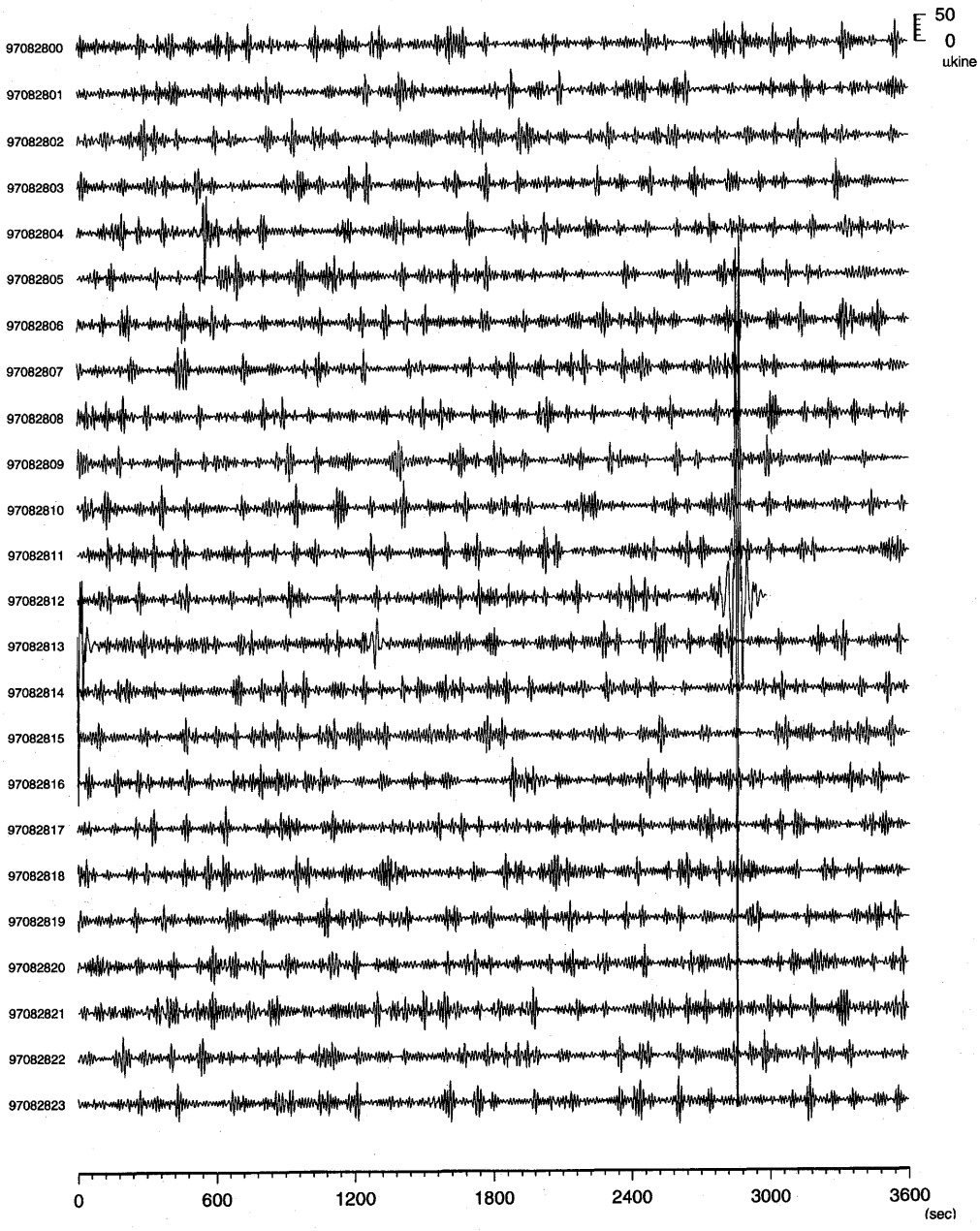
50
0
ukine
97082800
97082801
97082802
97082803
97082804
97082805
97082806
97082807
97082808
97082809
97082810
97082811
97082812
97082813
97082814
97082815
97082816
97082817
97082818
97082819
97082820
97082821
97082822
97082823
0
600
1200
1800
2400
3000
3600
(sec)

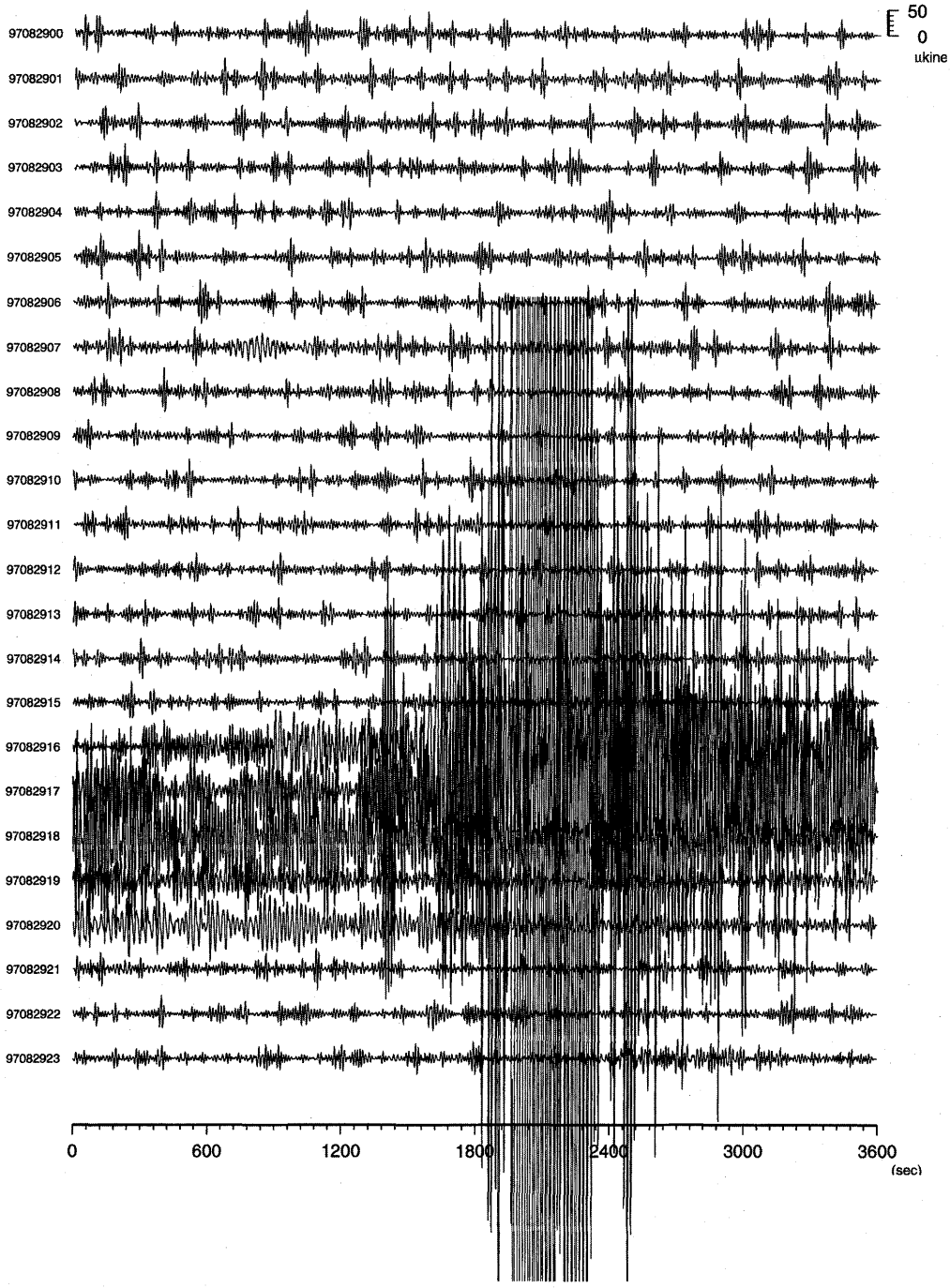
50
0
ukine
97082900
97082901
97082902
97082903
97082904
97082905
97082906
97082907
97082908
97082909
97082910
97082911
97082912
97082913
97082914
97082915
97082916
97082917
97082918
97082919
97082920
97082921
97082922
97082923
0
600
1200
1800
2400
3000
3600
(sec)